



## Molecular Crystals and Liquid Crystals Science and Technology. Section A. Molecular Crystals and Liquid Crystals

Publication details, including instructions for authors and  
subscription information:

<http://www.tandfonline.com/loi/gmcl19>

### Structural and Magnetic Properties of the Topologically Novel 2-D Material $\text{Cu}_9\text{F}_2\text{cpa})_6$ : A Triangulated Kagome - Like Hexagonal Network of Cu(II) Trimers Interconnected by Cu(II) Monomers

Michael Gonzalez <sup>a</sup>, Francisco Cervantes-lee <sup>a</sup> & Leonard W. ter  
Haar <sup>a</sup>

<sup>a</sup> Department of Chemistry, University of Texas, El Paso, TX,  
79968-0513, USA

Version of record first published: 05 Dec 2006.

To cite this article: Michael Gonzalez , Francisco Cervantes-lee & Leonard W. ter Haar (1993):  
Structural and Magnetic Properties of the Topologically Novel 2-D Material  $\text{Cu}_9\text{F}_2\text{cpa})_6$ : A Triangulated  
Kagome - Like Hexagonal Network of Cu(II) Trimers Interconnected by Cu(II) Monomers, Molecular  
Crystals and Liquid Crystals Science and Technology. Section A. Molecular Crystals and Liquid Crystals,  
233:1, 317-324

To link to this article: <http://dx.doi.org/10.1080/10587259308054973>

PLEASE SCROLL DOWN FOR ARTICLE

Full terms and conditions of use: <http://www.tandfonline.com/page/terms-and-conditions>

This article may be used for research, teaching, and private study purposes. Any  
substantial or systematic reproduction, redistribution, reselling, loan, sub-licensing,  
systematic supply, or distribution in any form to anyone is expressly forbidden.

The publisher does not give any warranty express or implied or make any representation  
that the contents will be complete or accurate or up to date. The accuracy of any  
instructions, formulae, and drug doses should be independently verified with primary  
sources. The publisher shall not be liable for any loss, actions, claims, proceedings,  
demand, or costs or damages whatsoever or howsoever caused arising directly or  
indirectly in connection with or arising out of the use of this material.

## STRUCTURAL AND MAGNETIC PROPERTIES OF THE TOPOLOGICALLY NOVEL 2-D MATERIAL $\text{Cu}_9\text{F}_2(\text{cpa})_6$ : A TRIANGULATED KAGOME - LIKE HEXAGONAL NETWORK OF $\text{Cu(II)}$ TRIMERS INTERCONNECTED BY $\text{Cu(II)}$ MONOMERS

MICHAEL GONZALEZ, FRANCISCO CERVANTES-LEE and  
LEONARD W. ter HAAR\*

*Department of Chemistry, University of Texas, El Paso TX 79968-0513, USA*

**Abstract**  $\text{Cu}_9\text{F}_2(\text{cpa})_6 \cdot x\text{H}_2\text{O}$  (cpa = carboxypentonic acid) has been synthesized, and characterized by x-ray diffraction. It is isomorphous with the Cl and Br congeners. Two coordinatively different  $\text{Cu(II)}$  ions comprise the unit cell: six  $\text{Cu}_{\text{trimer}}$  (square pyramidal) and three  $\text{Cu}_{\text{monomer}}$  (elongated octahedra). The six  $\text{Cu}_t$  ions form two exchange coupled trimeric clusters. Each of these trimers is bridged to three  $\text{Cu}_m$  sites; each  $\text{Cu}_m$  is connected to two trimers. The extended lattice is a hexagonal network with trimers at the vertices and  $\text{Cu}_m$  ions along the edges. Magnetic field-dependent magnetic susceptibility studies in the range 1.7 - 300 K demonstrate that the compound has a magnetic ground state which is highly field dependent at lower temperatures (<20K). The interconnected triangulation suggests spin frustration. Theoretical results for this type of lattice are unknown, but analogies can be drawn to the Kagomé lattice.

## INTRODUCTION

The connectivity patterns which define magnetic lattices represent a common meeting ground for chemists and physicists interested in molecular-based magnetic materials.<sup>1</sup> This arises because novel interconnection patterns ultimately lead to new insight concerning the fundamental nature of extended interaction mechanisms, as well as suggesting technologically advantageous magnetic structure types and applications. Magnetic lattices are described in terms of their topology: namely, what types of magnetic sites are involved (organic, inorganic, mono- vs. polynuclear, total spin value per site, spin anisotropy, etc.) and what is the nature of the pairwise interactions that interconnect the magnetic sites (number and type of nearest- or next-nearest neighbors, whether antiferro- or ferromagnetic, relative magnitudes, and the presence of exchange anisotropy - Ising, XY or Heisenberg). Indeed, designing extended magnetic lattices with prescribed topologies and properties is the challenge at hand.

In our lab, efforts have been aimed at using framework structures as candidates for investigating novel magnetic phenomena and particularly as magneto-optical

materials based on organic/inorganic 'composites' at the molecular level. Part of this strategy is based on the use of ligands that are rich in the number of ligating donor atoms. In the present paper, we report preliminary magnetic studies and structural data for the fluoride congener of a series of isomorphous compounds given by the formula  $\text{Cu}_9\text{X}_2(\text{cpa})_6 \cdot x\text{H}_2\text{O}$ , a triangulated hexagonal layer which represents a unique extension of the interconnection exhibited by the idealized Kagomé lattice. It is particularly interesting from the viewpoint of cyclic exchange and spin frustration.

## EXPERIMENTAL

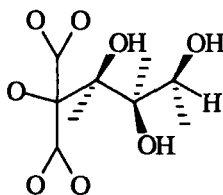
**Synthesis of  $\text{Cu}_9\text{F}_2(\text{cpa})_6 \cdot x\text{H}_2\text{O}$ .**  $\text{CuCl}_2 \cdot 2\text{H}_2\text{O}$  was reacted with ascorbic acid (2:1 mol ratio). The mixture was heated and allowed to stir until the precipitation of  $\text{CuCl}$  was complete (ca. 0.5 h), after which the  $\text{CuCl}$  was filtered off.  $\text{CuF}_2$  (1 mmol) was added to the clear solution followed by the addition 0.10 M NaOH to raise the pH to a value of 6. Blue hexagonal prisms were collected after 2-3 days. *Caution: HF is produced!*

**Crystal Structure Determination.** A blue hexagonal crystal (0.10 x 0.25 x 0.28) was mounted in a capillary with mother liquor and sealed. Crystal data were collected at room temperature on a R3m/V Nicolet four circle diffractometer with graphite monochromated  $\text{MoK}\alpha$  radiation;  $\lambda = 0.71073 \text{ \AA}$ . Unit cell parameters and standard deviations were obtained by least squares fit to 25 reflections randomly distributed in reciprocal space and lying in the range  $15 - 30^\circ$ . The structure was solved by full matrix least squares refinement using Shelxtl-Plus on a Microvax II. It is isomorphous with the Cl and Br derivatives.<sup>2</sup> *Crystal Data:*  $\text{C}_{36}\text{H}_{50}\text{F}_2\text{Cu}_9\text{O}_{51} \cdot x\text{H}_2\text{O}$  (unit cell contents), trigonal,  $P321$ ,  $a = b = 21.297(11)$ ,  $c = 7.965(10) \text{ \AA}$ ,  $V = 3128.6(4.9) \text{ \AA}^3$ , channels of disordered water (solvent) occupy ca. 40% of the unit cell.

**Magnetic susceptibility measurements.** Magnetic susceptibility data were collected in the temperature range 1.7 - 250 K using a Quantum Design SQUID-based magnetometer utilizing modifications and procedures described elsewhere.<sup>3</sup> Data were corrected for temperature independent magnetism ( $-556 \times 10^{-6}/\text{mol}$ ) using Pascal's constants<sup>4</sup> for the diamagnetic components and a T.I.P./Cu(II) of  $60 \times 10^{-6}$ . Figures in this paper are based on a molecular weight of 2603.1 g/mol (9 Cu(II)/unit cell).

## RESULTS

**Structural Description of  $\text{Cu}_9\text{F}_2(\text{cpa})_6 \cdot x\text{H}_2\text{O}$ .** 2-Carboxypentonic acid (cpa) is a polyhydroxypolycarboxylic acid obtained from the decomposition of ascorbic acid in the presence of Cu(II).<sup>5</sup> Its structure lends itself to a multitude of ligating possibilities in



which interconnected high-nuclearity species are readily envisaged. Two environments are found for the Cu(II) ions. The copper designated Cu<sub>trimer</sub> (Cu<sub>t</sub>) is near a crystallographic three fold axis and generates the trimeric unit shown in Figure 1. The

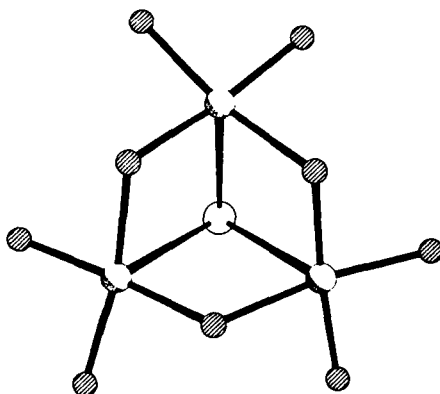


**FIGURE 1** Trimeric cluster of three square pyramidal Cu<sub>t</sub> ions.

ion has a square-pyramidal coordination sphere in which the basal sites are oxygen atoms from two different cpa anions, and the apical site is filled by a common  $\mu_3$ -fluoride ion located on the 3-fold axis. The Cu-O bridging network within the trimer is an alternating Cu<sub>3</sub>O<sub>3</sub> 'ring'; the Cu-O distances (2-hydroxy) are 1.92(2) - 1.94(2) Å.

Cu<sub>monomer</sub> (Cu<sub>m</sub>) is located on a crystallographic two-fold axis. It has four short Cu-O equatorial bonds and two longer Cu-O axial bonds; see Figure 2. Two carboxylate groups (of a single cpa) bridge the Cu<sub>m</sub> site to two Cu<sub>t</sub> sites; all relevant Cu-O distances are in the range 1.91(3) - 1.97(3). As shown in Figure 2, three such Cu<sub>m</sub> sites are connected to every Cu<sub>t</sub> based trimer; two trimers are connected to each Cu<sub>m</sub>. The axial positions of the six coordinate Cu<sub>m</sub> sites are occupied by the 3-hydroxy groups of two different cpa anions; these Cu-O distances are 2.29(4) Å.

To further develop the extended lattice structure, the fragment shown in Figure 2 is repeated so as to form a polymeric sheet which grows in the ab-plane. Figure 3 emphatically demonstrates that the sheet is a result of Cu-O, C-O and C-C bonding. The layer shown in Figure 3 stacks in the c direction; the layers are held together by

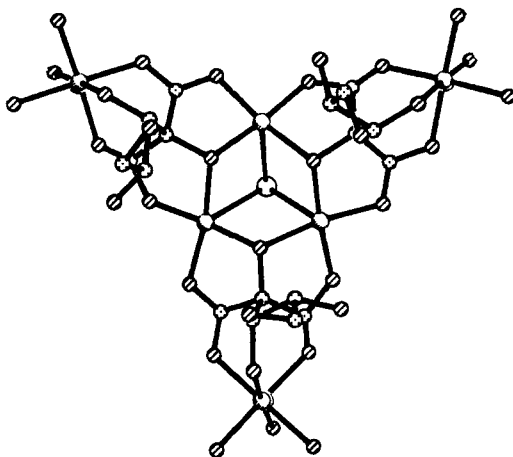


**FIGURE 2** The trimeric cluster (of Figure 1) bridged to three  $\text{Cu}_m$ .

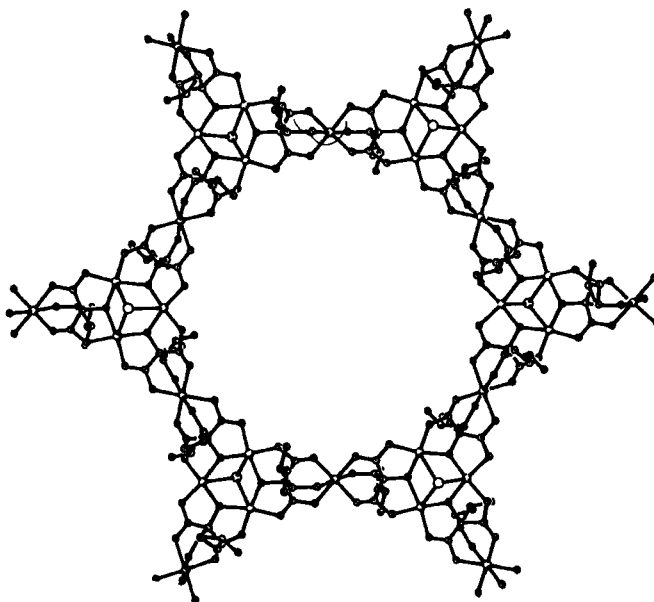


**FIGURE 3** The infinite layer structure and hexagonal columnar channels.

interactions involving extensive hydrogen bonding. The vertical stacking of the layers results in channels that pass through the crystals. These channels are *ca.* 20 Å in diameter and are occupied by water; channel volume is nearly 40% of the unit cell.

**Magnetic Susceptibility.** Susceptibility data were collected with applied magnetic fields in the range 1.0 G to 10 kG in the temperature range 1.7 to 300 K. The data are plotted in Figures 4 and 5 as  $\chi_m$ ,  $1/\chi_m$ , and  $\mu_{\text{eff}} = 2.828(\chi_m T)^{1/2}$ ; the molar basis is per

unit cell  $(\text{Cu}_9\text{F}_2(\text{cpa})_6 \cdot x\text{H}_2\text{O})$ . Several dominant features are noteworthy. In Figure 4, it is clearly seen that  $\chi_m$  diverges at low temperatures; it does not exhibit a maximum as a function of temperature. Although  $\mu_{\text{eff}} = 3.8$  B.M. at 300 K, it reaches a minimum (2.8 B.M.) near 60 K and a maximum (4.7 B.M.) near 6.8 K.

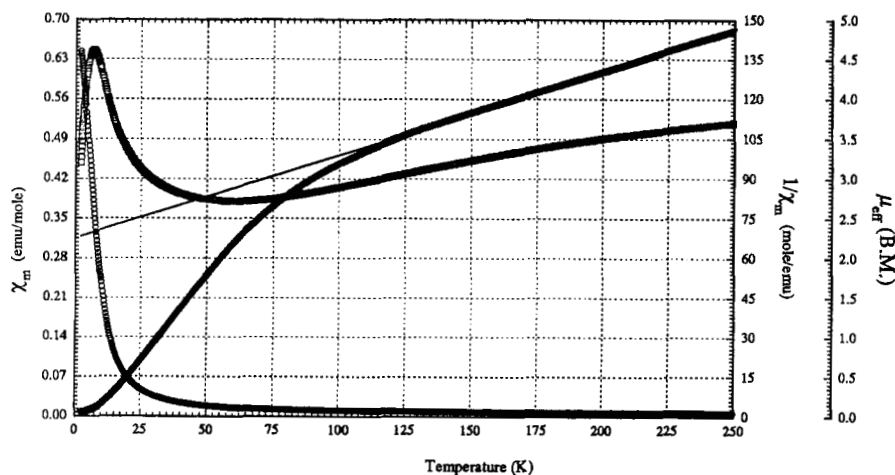


FIGURE 4 Magnetic data ( $\circ - \chi_m$ ,  $\nabla - 1/\chi_m$ ,  $\square - \mu_{\text{eff}}$ );  $H = 10,000$  G.

The  $1/\chi_m$  plot exhibits three distinct regions: for  $T > 150$  K, the data are linear as a function of temperature and can be fit by the Curie Weiss law,  $\chi_m = C/(T-\theta)$ , with parameters  $C = 3.193$  and  $\theta = -215.8$  K; for  $50 < T < 150$  K, the slope of the  $1/\chi_m$  curve changes continuously and it is not appropriate to use a Curie Weiss fit; for

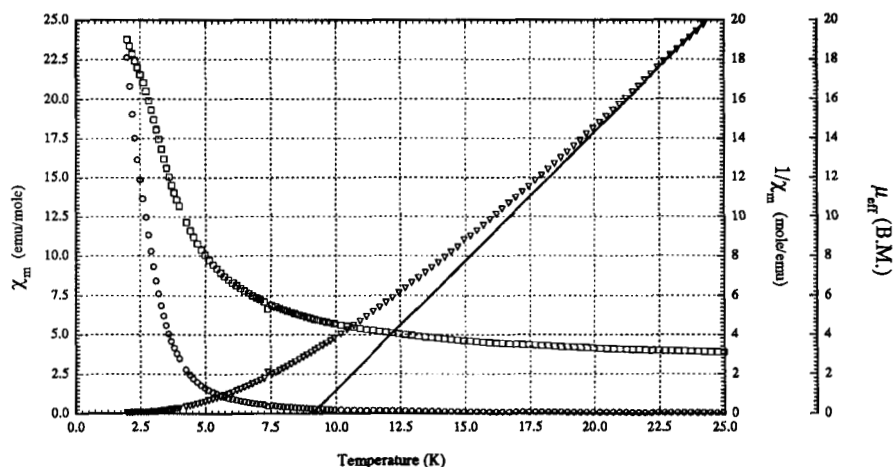


FIGURE 5 Magnetic data ( $\circ - \chi_m$ ,  $\nabla - 1/\chi_m$ ,  $\square - \mu_{\text{eff}}$ );  $H = 10$  G.

20 < T < 50 K, the  $1/\chi_m$  curve is again nearly linear and the best-fit Curie-Weiss parameters are  $C = 0.7618$  and  $\theta = +9.3$  K (this is the best-fit that is compared to the low-field data in Figure 5). Below 20 K the data become increasingly field dependent and exhibit a marked increase in the susceptibility and moment values.

For  $T > 125$  K, and using an average g-value of 2.1 for Cu(II), the S value per unit cell formula is clearly reduced with respect to the value expected for nine moles of noninteracting paramagnetic  $S = 1/2$  ions.<sup>4</sup> Such a reduction in S value is in agreement with the decreasing value of  $\mu_{\text{eff}}$  and is indicative of the very strong antiferromagnetic exchange interactions that are suggested by  $\theta = -215.8$  K. At high fields, the  $\mu_{\text{eff}}$  plot clearly indicates that a minimum spin value is reached before a rounded maximum occurs upon further cooling. The temperature at which such a rounded maximum occurs in  $\mu_{\text{eff}}$  is highly dependent on the applied field; the maximum shifts to lower temperatures with smaller applied fields. The low-field data in Figure 5 clearly demonstrate this feature -  $\mu_{\text{eff}}$  reaches a maximum value of over 19 B.M. at 1.7 K whilst it is clear that a maximum has yet to be realized, perhaps at lower temperatures.

## DISCUSSION

The extended structure of  $\text{Cu}_9\text{X}_2(\text{cpa})_6 \cdot x\text{H}_2\text{O}$  is clearly unique, particularly among layered magnetic materials. This stems from several reasons. *First*, it is quite clear that the chemical lattice shown in Figure 3 must correspond to the magnetic network, or

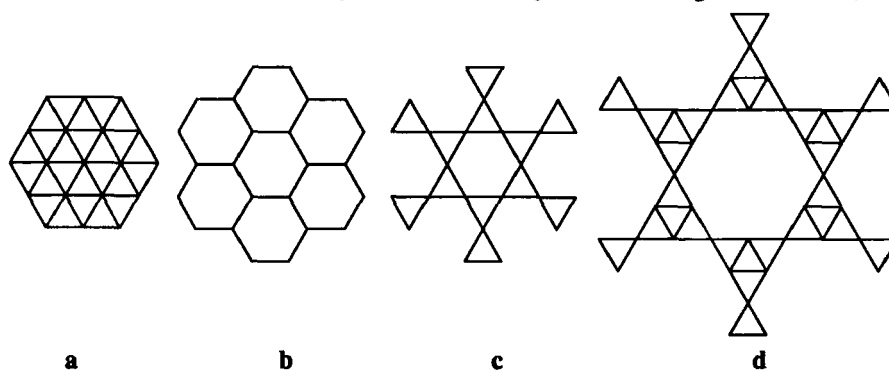


FIGURE 6 a) triangular, b) honeycomb, c) Kagomé, d)  $\text{Cu}_9\text{F}_2(\text{cpa})_6 \cdot x\text{H}_2\text{O}$

connectivity pattern, displayed in Figure 6d, where the solid lines represent possible superexchange pathways and the points of intersection are spins. Careful comparison to other triangulated lattices currently of interest (Figures 6a-c) emphasizes a number of topological similarities and differences.<sup>6</sup> *Second*, triangulated spin systems are

notable for the spin frustration they may exhibit. A large number of triangular clusters are already known.<sup>7</sup> More to the point however, extended lattices which consist of interconnected, possibly frustrated, triangulated units have heretofore not been reported for molecular-based magnetic materials. In fact, the  $\text{Cu}_9\text{X}_2(\text{cpa})_6 \cdot x\text{H}_2\text{O}$  lattice suggests a new direction for the design and synthesis of novel magnetic materials. *Third*, triangulated magnetic lattices are of particular interest as experimental testing grounds for the physics associated with degenerate ground states and finite entropies (at  $T = 0$ ).

Chemically, the  $\text{Cu}_9\text{X}_2(\text{cpa})_6 \cdot x\text{H}_2\text{O}$  magnetic lattice consists of two different spin sites and two exchange parameters. There are twice as many  $\text{Cu}_t$  sites as there are  $\text{Cu}_m$  sites. Each  $\text{Cu}_t$  site is connected by superexchange pathways to two other  $\text{Cu}_t$  sites within the same trimeric unit. Each  $\text{Cu}_t$  site is also connected by two separate but crystallographically equivalent superexchange pathways to two  $\text{Cu}_m$  sites. Each  $\text{Cu}_m$  site is connected by four such pathways to four equivalent  $\text{Cu}_t$  sites (alternately speaking, two trimers). Topologically, the pairwise exchange interactions between  $\text{Cu}_t$  sites is equal in value and we refer to it as the *intratrimer* exchange parameter. The trimeric units are interconnected to one another by way of four pairwise exchange interactions inbetween four  $\text{Cu}_t$  sites on two trimers and the  $\text{Cu}_m$  site that interconnects the two trimers. We refer to each of these exchange interactions as the *intertrimer* parameter. The intratrimer exchange parameter is likely to be large in magnitude and antiferromagnetic in nature because of the alkoxy bridging oxygens in the  $\text{Cu}_3\text{O}_3$  ring and, to a much lesser extent, the tri-bridging fluoride.<sup>8</sup> (To the best of our knowledge, tri-bridging fluorides are extremely rare in  $\text{Cu(II)}$  systems.) The intratrimer exchange is likely responsible for the large  $\theta$  value observed in the high temperature data. With a large antiferromagnetic intratrimer/intertrimer exchange ratio, the trimers could in principle behave as effective  $S = 1/2$  magnetic entities, resulting in *five*  $S = 1/2$  sites per  $\text{Cu}_9\text{X}_2(\text{cpa})_6 \cdot x\text{H}_2\text{O}$  unit cell. This is in agreement with the gradually increasing  $\mu_{\text{eff}}$  value of 3.8 - 4.0 B.M. (calculated for five moles of noninteracting  $S = 1/2$  sites per MW unit). Such a model is more accurately depicted by the network schematic shown in Figure 7, where the magnetic lattice could be treated as a honeycomb-type lattice in which effective  $S = 1/2$  spin sites are located at the vertices *and along the edges*.

There is presently a great deal of interest in topologically frustrated systems.<sup>9</sup> On the theoretical side, this stems in part from Anderson's resonating valence bond structure for superconductivity in doped cuprates.<sup>10</sup> One feature of the liquidlike RVB state is the absence of long-range order in the ground state. Similar results for cooperative spins on frustrating lattices can also be obtained. Although good experimental examples of either have not yet been found in real magnetic materials, a few compounds have been found to exhibit a number of novel low-temperature states



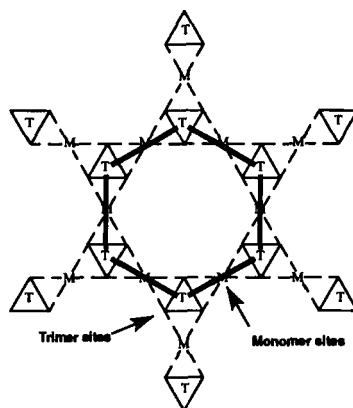


**FIGURE 7** Alternate schematic in which strongly antiferromagnetic trimers are a single site.

that may be associated with frustration. The Kagome lattice, in particular, can display 'order from disorder' -- the order being spin nematic. The KL has been proposed<sup>6</sup> as a model for  $^3\text{He}$  adsorbed on graphite ( $S = 1/2$ ) and for the insulating layered compound  $\text{SrCr}_8\text{Ga}_4\text{O}_{19}$  ( $S = 3/2$ ). Given the possibility that such novel states may also occur in other triangulated lattices, further study of the  $\text{Cu}_9\text{X}_2(\text{cpa})_6$  compounds is certainly warranted. Additional synthetic work and magnetic characterization is in progress.

## ACKNOWLEDGMENTS

This research was supported by the National Science Foundation and AT&T Bell Labs, as well as financial support from the DOD-DLA for the SQUID magnetometer.

## REFERENCES

- <sup>1</sup> D. Gatteschi, O. Kahn, J.S. Miller, F. Palacio, Eds., *Magnetic Molecular Materials*, Kluwer Academic Publishers: Dordrecht, The Netherlands, (1991).
- <sup>2</sup> R.E. Norman, N.J. Rose, R.E. Stenkamp, *J. Chem. Soc. Dalton Trans.*, 2905 (1987); R.E. Norman, R.E. Stenkamp, *Acta Cryst.* C46, 6 (1990).
- <sup>3</sup> D. Nelson, L.W. ter Haar, *Inorg. Chem.*, (1992), in press.
- <sup>4</sup> E.A. Boudreaux, L.N. Mulay, Eds., *Theory and Applications of Molecular Paramagnetism*, John Wiley and Sons: New York, (1976).
- <sup>5</sup> G. Wilkinson, *Comprehensive Coordination Chemistry*, Vol. 5, Pergamon, (1987), 450ff.
- <sup>6</sup> See e.g., D.A. Huse and V. Elser, *Phys. Rev. Lett.* **60**, 2531 (1988); V. Elser, *Phys. Rev. Lett.* **62**, 2405 (1989); X. Obradors, A. Labarta, A. Isalgué, J. Tejada, J. Rodriguez, and M. Pernet, *Solid State Commun.* **65**, 189 (1988); A. P. Ramirez, G.P. Espinosa, A.S. Cooper, *Phys. Rev. Lett.* **64**, 2070 (1990).
- <sup>7</sup> J.K. McCusker, H.G. Jang, S. Wang, G. Christou, D.N. Hendrickson, *Inorg. Chem.* **31**, 1874 (1992), and references therein.
- <sup>8</sup> O. Kahn, *Angew. Chem. Int. ed. Engl.* **24**, 834 (1985), and references therein.
- <sup>9</sup> J.T. Chalker, P.C.W. Holdsworth, E.F. Shender, *Phys. Rev. Lett.* **68**, 855 (1992); A.B. Harris, A. J. Berlinsky, C. Bruder, *J. Appl. Phys.* **69**, 5200 (1991).
- <sup>10</sup> P.W. Anderson, *Science*, **235**, 1196 (1987).